Geophys. J. Int. (2001) **145,** 277–290

Electromagnetic induction information from differences at aeromagnetic crossover points

A. P. Hitchman,[1] F. E. M. Lilley[1] and P. R. Milligan[2]

[1] *Research School of Earth Sciences, Australian National University, Canberra* ACT 0200*, Australia*
[2] *Australian Geological Survey Organisation,* PO Box 378, *Canberra* ACT 2601, *Australia*

Accepted 2000 November 14. Received 2000 November 6; in original form 1999 October 21

SUMMARY

This paper describes an investigation of the use of aeromagnetic crossover misfits as a source of geological information. The misfits occur when, at a crossover point of an aeromagnetic survey, the separate measurements of the Earth's magnetic field are not the same. Misfits are mainly the result of time-dependent field changes and, in this paper, are analysed as indicators of electromagnetic induction in the Earth, and thus of electrical conductivity structure. The method derives estimates of a magnetic diurnal variation function both for cells within the surveyed area and for a reference base station. Normalizing the former by the latter gives extra information from the aeromagnetic data. A case history from Australia is presented of the method applied to an aeromagnetic survey conducted in a region containing a known electrical conductivity structure. The presence of the conductivity anomaly is evident in the aeromagnetic misfit results.

Key words: aeromagnetic crossover misfits, electrical conductivity, electromagnetic induction, geomagnetism, total magnetic field.

1 INTRODUCTION

An aeromagnetic survey seeks to obtain an optimum representation of the space-dependent crustal magnetic anomaly field. Time variations of the magnetic field are generally present during survey measurements, and it is necessary to remove their effects from an observed aeromagnetic data set. For this purpose, aeromagnetic surveys commonly consist of both survey lines and more widely spaced ties, flown at right angles to these lines (see Fig. 1). This practice gives rise to crossover points where lines and ties intersect and two separate measurements of the total magnetic field have been made. Usually the line and tie measurements are different so that a misfit exists at the crossover point.

The basic method for eliminating time variations from aeromagnetic data is levelling, using this misfit information (Luyendyk 1997). Levelling smoothes the effects of the misfits by distributing them about a closed loop of crossover points (Green 1983). Alternatively, misfits along a line or tie can be represented as a polynomial, which is subtracted from the data (Yarger *et al.* 1978).

Because aeromagnetic misfits may be expected to contain a component due to fields induced in the Earth by magnetic variations with time, the misfits are data of opportunity for studying electromagnetic induction in the Earth. The present paper investigates what can be gleaned from them, notwithstanding the fact that a designed crossover-misfit experiment might produce data that are more ideal. The objective is to gain reconnaissance information on regional electrical conductivity structure for an area where an aeromagnetic survey has been carried out. Such information may lead to, and help focus, further and more detailed electromagnetic ground work. That misfits may exhibit a space dependence above geological settings where the electrical conductivity structure is heterogeneous was pursued earlier by Le Borgne & Le Mouël (1975) and Achache (1977).

In the past, other effects have contributed to aeromagnetic misfits in addition to field changes with time, especially navigation errors and altitude differences (Luyendyk 1997). However, in modern aeromagnetic surveys the use of differential GPS navigation systems has greatly reduced positioning errors, so that the most significant contribution to misfits is now from time-dependent field changes (Reeves 1993). The availability of a great deal of high-resolution aeromagnetic data, with accurate navigation and magnetic readings, has stimulated the present research.

In addition to levelling, a second method for eliminating time variations from aeromagnetic data uses the time-varying magnetic field recorded at the base station (Reeves 1993). The base-station record is subtracted from the aircraft record, on the assumption that the time-varying field is uniform across the survey area (including the base-station location). A difficulty of this method is that while there are many areas where the assumption holds true, there are also many areas where it is

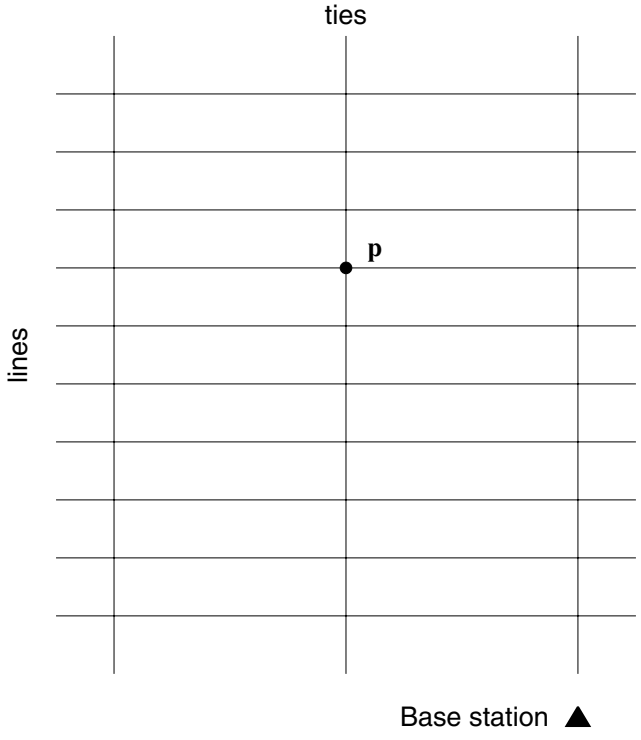

Figure 1. During an aeromagnetic survey a series of lines and ties is flown over the survey area. The result is a large number of crossover points, such as **p**, at which the total magnetic field has been measured at two different times. A fixed base station is commonly used to record time variations at a location within or close to the survey area.

contravened, particularly near heterogeneous electrical conductivity structure (see e.g. Lilley 1982; Milligan & Barton 1997). The use of multiple base stations to monitor the spatial dependence of time variations across a survey area has been investigated and demonstrated by Whellams (1996), who deployed an array of 36 base stations during an aeromagnetic survey in South Australia. However, the practice of multiple base-station surveys is in its infancy, and typical contemporary aeromagnetic surveys use a single base station in conjunction with both lines and ties.

The electrical conductivity structure near the base station will clearly have a major influence on the results of procedures described below. While consideration of electrical conductivity structure (and especially the presence of conductivity anomalies) is increasingly advocated as important in siting aeromagnetic base stations, logistic factors such as ease of access are often paramount. Thus, a base station of opportunity may or may not be in a suitable position, electromagnetically speaking. In the case study presented in Section 5, the base station is in a region earlier covered by a magnetometer array study (Gough *et al.* 1974). The base-station site, Broken Hill, is known to be to the east of a major conductivity anomaly.

In the context of the present work it is also relevant to mention the effect examined by Schmidt *et al.* (1993) and Clark *et al.* (1998). In this effect the induced (as opposed to the remanent) component of the crustal magnetization changes with the ambient magnetic field, and so changes, for example, during the normal daily magnetic variation. The detection of such an effect is, however, not considered to be within the scope of the methods outlined below, and the effect is not discussed further in the present paper.

2 OUTLINE OF PROCEDURE

In order to determine if characteristics of the misfit data have a space dependence over an aeromagnetic survey area, the area is divided into cells. In the case study presented below, the magnetic survey area is some 160 km square and it is divided into a regular grid of cells, each approximately 40 km square. Each crossover misfit has a geographic position, and those misfits located within a particular cell are spatially binned into that cell. Each cell then contains approximately 1000 crossover data.

The crossover misfits in each cell are used to recover a diurnal function, which is representative of the magnetic variations with time occurring in that cell area. This diurnal function is a weighted average of the daily variations that take place during the flying of the lines and ties that cross the cell.

A supplementary base-station data set is constructed by differencing the base-station measurements at the times a line, and separately a tie, traverse each crossover point in the survey area. Adjustments to times are made to allow for the variation of local solar time with longitude. For every aircraft-observed misfit, a corresponding base-station misfit is thus obtained. A reference diurnal function for each cell is then computed using the base-station misfit data that correspond to the aircraft-misfit data for that particular cell.

Hence, two diurnal functions are associated with each cell of the survey area. The first is obtained using misfits measured by the aircraft when within the cell, and the second, a reference function, is derived from base-station records using misfits reconstructed for the same (adjusted) times.

Mapping these differences allows the spatial variability of the time-varying field across the survey area to be analysed and an EM-dependent image of the survey area to be produced. This EM-dependent image is in addition to the image of crustal magnetization, which is the normal product of an aeromagnetic survey.

In this paper the comparison of the aircraft and base-station diurnal functions is treated in two ways. In the first, a residual index is computed, based on the difference between rms aircraft and base-station indices derived from the respective diurnal functions. In the second, a linear relationship between the two functions is sought, to give a coefficient of proportionality between them. The development of these two quantitative indices is described in Section 4.

3 METHODS FOR RECOVERING A DIURNAL FUNCTION

Two approaches have been taken to compute a diurnal function from crossover misfits. The first approach uses a Fourier series to represent the magnetic variation with time. The second approach, termed data binning, groups misfits into time bins according to the times at which their associated lines and ties were flown.

Both approaches result in mathematical expressions for the diurnal function that involve a series of unknown parameters. The known crossover misfits are the data from which the unknown parameters are determined. Generally the number of misfits is very much greater than the number of unknowns, and it is possible to obtain a representative diurnal function by solving an overdetermined problem. In the examples presented in Sections 6 and 7, the overdetermined systems of linear

equations for both the Fourier series and data-binning methods are solved using the singular value decomposition method of Press *et al.* (1992, Section 15.4).

3.1 Fourier series

The total-field magnetic variation, $F(t)$, may be expressed generally as a Fourier series,

$$F(t) = a_0 + \sum_{n=1}^{\infty} (a_n \sin \omega_n t + b_n \cos \omega_n t) , \quad (1)$$

where a_0, a_n and b_n ($n = 1, \ldots, \infty$) are the Fourier coefficients, ω is the angular frequency and t is time.

At a crossover point in an aeromagnetic survey, say **p** in Fig. 1, the time-dependent total field is measured on two occasions, once while flying the line (at time t_L) and once while flying the tie (at time t_T). If β is used to represent the misfit between the line and tie measurements, then

$$\beta = F(t_L) - F(t_T) . \quad (2)$$

Taking the field to be represented by eq. (1), eq. (2) can be written as

$$\beta = \sum_{n=1}^{\infty} [a_n(\sin \omega_n t_L - \sin \omega_n t_T) + b_n(\cos \omega_n t_L - \cos \omega_n t_T)] . \quad (3)$$

The difference of the two magnetic field values recorded by the aircraft at point **p** thus gives one equation of the form of eq. (3).

To describe the daily variation for magnetically quiet days, it is common to take just the terms for the baseline value (a_0) and the first four harmonics of a day (Parkinson 1983). This truncation at four harmonics is now adopted here to emphasize the quiet daily variation part of the magnetic variation spectrum, and to filter out signals of shorter period.

To the extent that all crossover points within a cell have experienced a repetitive magnetic daily variation, each crossover datum will generate an equation of the form of eq. (3) (as truncated). For more than eight crossover points in a cell, the linear system of equations becomes overdetermined and can be solved for the eight Fourier coefficient values. These coefficient values as determined will be denoted a_n^a and b_n^a ($n = 1, \ldots, 4$), where the superscript 'a' indicates values determined from aircraft data.

A diurnal function, $\mathscr{F}^a$, derived from aircraft data collected within a cell, is now defined as

$$\mathscr{F}^a(t) = \sum_{n=1}^{4} (a_n^a \sin \omega_n t + b_n^a \cos \omega_n t) . \quad (4)$$

Note that a_0 is not determined by this approach. This circumstance is unimportant, however, as the steady component of the magnetic field does not contribute to relevant electromagnetic induction phenomena. Hence, all recovered variations shown in Figs 4 to 7 are drawn with arbitrary baselines.

For each misfit datum of the form of eq. (2), a corresponding equation is also constructed using the base-station data. Denoting the total-field magnetic variation at the base station by $F^b(t)$, the base-station values at the times the line and tie overfly point **p** will be $F^b(t_L)$ and $F^b(t_T)$. The corresponding base-station misfit β^b is thus constructed as

$$\beta^b = F^b(t_L) - F^b(t_T) . \quad (5)$$

The procedure followed for the aircraft data within a cell is then followed for the base-station data for that cell. An overdetermined set of linear equations is generated and solved for Fourier coefficients for the base station, a_n^b and b_n^b. A base-station diurnal function, $\mathscr{F}^b(t)$, is then constructed for each cell according to

$$\mathscr{F}^b(t) = \sum_{n=1}^{4} (a_n^b \sin \omega_n t + b_n^b \cos \omega_n t) . \quad (6)$$

Because further computations concerning the diurnal functions $\mathscr{F}^a(t)$ and $\mathscr{F}^b(t)$ involve discrete time-series, the functions are evaluated at intervals of 1 min over the periods for which misfit data are held, according to eqs (4) and (6). The time-series thus generated, of M points, will be denoted $\mathscr{F}_j^a$ and $\mathscr{F}_j^b$ for $j = 1, \ldots, M$.

The above method (but without base-station data) is similar to one used by Sander & Mrazek (1982) to recover a daily variation from misfits in marine magnetic data. However, whereas marine magnetic data may be observed continuously, night and day, aeromagnetic data are generally restricted to daytime. Fourier coefficient values obtained from aeromagnetic data using the method described above are thus without night-time control. However, the time-series generated by the recovered Fourier coefficients in combination are regarded as providing useful representations of the actual daily variation during times with good crossover control (but see the comment in Section 4.3 regarding errors arising in the Fourier method).

3.2 Data binning

In the data-binning method the period of daytime for which there are misfit data is divided into J equal time intervals or bins. Bin length is governed by the number and distribution of the misfit data, and in the present work is generally 1 hr, with bins corresponding to complete hours of local time. The total-field variation $F(t)$ is then represented by a discrete series of hourly values, F_j, where $j = 1, \ldots, J$. Thus there is one total-field value per hourly bin. Consistent with the concept of a repetitive magnetic daily variation, the same discrete hourly series is taken to apply to each day.

Each crossover misfit is taken to represent a relationship between two bins: those during which the line and tie measurements were made. Misfits are discarded if the line and tie times are in the same bin. Eq. (2) is approximated by the form

$$\beta = F_{j_L} - F_{j_T} , \quad (7)$$

where subscripts j_L and j_T denote the bins during which the line and tie, respectively, were flown over **p**. Each misfit datum then gives an equation with the form of eq. (7). When the equations generated by the misfit data for all the crossover points within a particular cell are taken together, an overdetermined set of linear equations is again obtained for the unknowns F_j.

When solved for a particular cell, a discrete time-series has been determined directly that is equivalent to the diurnal function introduced above, and that will be denoted here as $\mathscr{F}_j$, $j = 1, \ldots, J$. Note that due to the difference nature of eq. (7), an arbitrary constant can be added to both F_{j_L} and F_{j_T} without changing the value of β. Thus each time-series $\mathscr{F}_j$ is

also determined relative to an arbitrary zero level. For each cell of the survey area, the time-series derived from aircraft data will be designated $\mathscr{F}_j^{\mathrm{a}}$ and that derived from base-station data $\mathscr{F}_j^{\mathrm{b}}$, as before.

Note that whereas the Fourier method will have a low-pass filtering effect on the data due to the truncation of its harmonics, in the binning method a low-pass filtering effect is imposed by the length of bin.

3.3 Zero levels

A diurnal function specified according to eq. (4) or eq. (6) will automatically have a zero mean value if evaluated over a full day. However, if evaluated over part of a day, this condition will not apply. Therefore, where such diurnal functions have been evaluated over some part of a day, their zero levels have been re-set to maintain zero mean values for those functions.

The series of hourly values obtained by the data-binning method are returned by the algorithm used with their zero levels adjusted such that their mean values are zero. Diurnal functions obtained by data binning thus automatically have zero mean value.

4 THE QUANTITATIVE INDICES

4.1 The residual index

Rms values, ψ and Ψ, of diurnal functions $\mathscr{F}_j^{\mathrm{a}}$ and $\mathscr{F}_j^{\mathrm{b}}$ (whether determined by the Fourier coefficient or data-binning method) have then been determined as

$$\psi = \sqrt{\frac{1}{J}\sum_{j=1}^{J}(\mathscr{F}_j^{\mathrm{a}})^2} \tag{8}$$

and

$$\Psi = \sqrt{\frac{1}{J}\sum_{j=1}^{J}(\mathscr{F}_j^{\mathrm{b}})^2}\,. \tag{9}$$

The residual index, η, for the cell to which $\mathscr{F}^{\mathrm{a}}(t)$ applies is then defined as

$$\eta = \psi - \Psi\,. \tag{10}$$

The residual index thus indicates enhancement (when positive) or reduction (when negative) of the strength of the aircraft diurnal function relative to the base-station function.

A residual time-series may also be obtained for each cell by subtracting, point by point, the base-station diurnal function from the aircraft diurnal function. Some such difference functions are included in plots of diurnal functions below. Because at the time of this point-by-point subtraction both diurnal functions will have zero mean values, the difference function will also have a zero mean value.

The approach taken here has some similarity to that of Fanselau (1968), who used the amplitude range of variations in the vertical component of the magnetic field to delineate conductivity structure. Fanselau subtracted the range of a base-station variation from the range of variations recorded at other ground stations, and interpreted changes in the sign of this quantity as an indication of the location of a conductivity contrast. A similar interpretation can be attached to the pattern in the rms index of the diurnal residual in the present work.

4.2 The diurnal ratio

A second way of comparing the recovered aircraft and base-station functions for each cell is by means of the ratio of their amplitudes. As a measure of such a ratio, a transfer function A is determined by linear regression between the time-series $\mathscr{F}_j^{\mathrm{a}}$ and $\mathscr{F}_j^{\mathrm{b}}$, such that

$$\mathscr{F}_j^{\mathrm{a}} = A\,\mathscr{F}_j^{\mathrm{b}}, \qquad j = 1, \ldots, M\,. \tag{11}$$

Such a relationship can be shown graphically by a plot of aircraft function against base-station function, point by point. The (positive) gradient of the straight line fitted to such a plot is then the ratio of the amplitudes of the two diurnal functions.

Enhancement of the aircraft function relative to the base-station function gives an A value greater than unity, and reduction gives an A value less than unity. For convenience, in the remainder of this paper the practice has been adopted of multiplying A by a factor of 100 to give an index that measures the amplitude of the aircraft function as a percentage of the base-station function.

Riddihough (1971) used an approach similar to that above to compare total-field variations across the British Isles. Ravat *et al.* (1995) and Langel & Whaler (1996) used a similar transfer function approach to compare, spatially, the amplitudes of different satellite-derived maps of the magnetic anomaly field.

4.3 Errors

The basic error in individual measurements of the total magnetic field in the case study below is taken as ± 1 nT (Luyendyk 1997). As the magnetometer used is inherently more accurate than this figure would suggest, this error estimate also allows for matters such as navigation precision, when two aircraft measurements are regarded as being at the same geographic point. Because a misfit at a crossover point is the result of subtracting one field measurement from another, the error estimate for a misfit is taken to be 1.5 nT.

When the diurnal functions $\mathscr{F}_j^{\mathrm{a}}$ and $\mathscr{F}_j^{\mathrm{b}}$ for $j = 1, \ldots, M$ are computed, standard errors are recovered for the Fourier coefficients in the first method and for the data bins in the second method. Thus standard errors are known for each member of those discrete series. For convenience, a representative error for any member of a series is calculated by taking the arithmetic mean of the individual errors for the members of the whole series.

These errors are denoted σ_a and σ_b for the aircraft and base-station diurnal functions, respectively, and values for them are included in the diurnal plots Figs 6 and 7. Also in these figures, a standard error σ_{d} for each member of a difference diurnal function is given. Once standard errors are known for the diurnal functions, established error theory is used to carry errors through to the estimation of the residual index values and the diurnal ratios, as presented in Fig. 9.

For the data-binning results this procedure for error computation appears to work in a straightforward manner, and error values are obtained that appear reasonable. For the Fourier coefficient method the error estimates obtained are large, perhaps reflecting the unsuitability of the method for data that have no night-time control. The authors considered omitting the Fourier method results from the present paper but have kept them in, for the interest of their comparison with the data-binning results.

5 DATA DESCRIPTION: THE FROME AEROMAGNETIC SURVEY

The case study presented in this paper is that of the Frome aeromagnetic survey (Richardson 1996), flown by the Australian Geological Survey Organisation (AGSO). The area of the Frome survey is topographically very flat. This circumstance brings the benefit that the survey aircraft can more easily fly at a constant altitude, reducing the contribution to misfit values that can come from line and tie values being observed at different altitudes. Fig. 2 shows the survey location in South Australia. Table 1 gives the survey specifications.

In the survey, total-field magnetic measurements were made simultaneously at the aircraft and at a base station by two optically pumped helium-vapour magnetometers, sampling every 0.1 s (Richardson 1996). Navigation data were obtained using a differential GPS system, giving horizontal aircraft location to better than 5 m (Horsfall 1997). These survey data yield 16 301 misfit values, which are discussed separately in Appendix A.

Table 1. Specifications for the Frome aeromagnetic survey (Richardson 1996; Mitchell *et al.* 1997).

Dates	3/8/95–25/11/95
Longitude range	139.5°E–141.0°E
Latitude range	29.5°S–31.0°S
Line spacing	400 m
Tie spacing	4000 m
Total distance	68 300 km
Line direction	E–W
Altitude	80 m
Base station	141°27°57.6″E, 32°00°0.0″S

The Frome aeromagnetic survey overlies, in part, the Flinders conductivity anomaly (FCA). The location of the FCA has been established previously by magnetometer array studies (see e.g. Gough *et al.* 1974; White & Polatayko 1985; Chamalaun 1985). At the longer periods of the daily variation, the array data of Gough *et al.* (1974) have been analysed by Lilley (1975), and the conclusion drawn that the FCA is also evident at these long periods.

The most recent of these studies is that of Paul (1994), whose anomaly location using magnetic field variations with period 1 hr is reproduced in Fig. 2. The analysis of the crossover misfits of the Frome aeromagnetic survey in this paper is thus intended to test the sensitivity of the misfits to the induction effects of a major electrical conductivity anomaly.

It is also appropriate to note that the year of the Frome survey, 1995, was a time of low solar activity, and so was a geomagnetically quiet year. 1995 is regarded as being the last year of Solar Cycle number 22, with Cycle number 23 starting in 1996 (Campbell 1997). Solar activity is relevant, as the methods described in this paper might be expected to work best for days of quiet magnetic variation that are undisturbed by storm activity.

On this point, it is appropriate to note further that the region of the Frome survey lies just north of a band across the Australian continent that has been described as 'amphidromic' by Lilley *et al.* (1999), due to the suppression there of magnetic activity as recorded by total-field instruments. The reason for the suppression is widespread destructive interference between the contributions of the north-horizontal and vertical

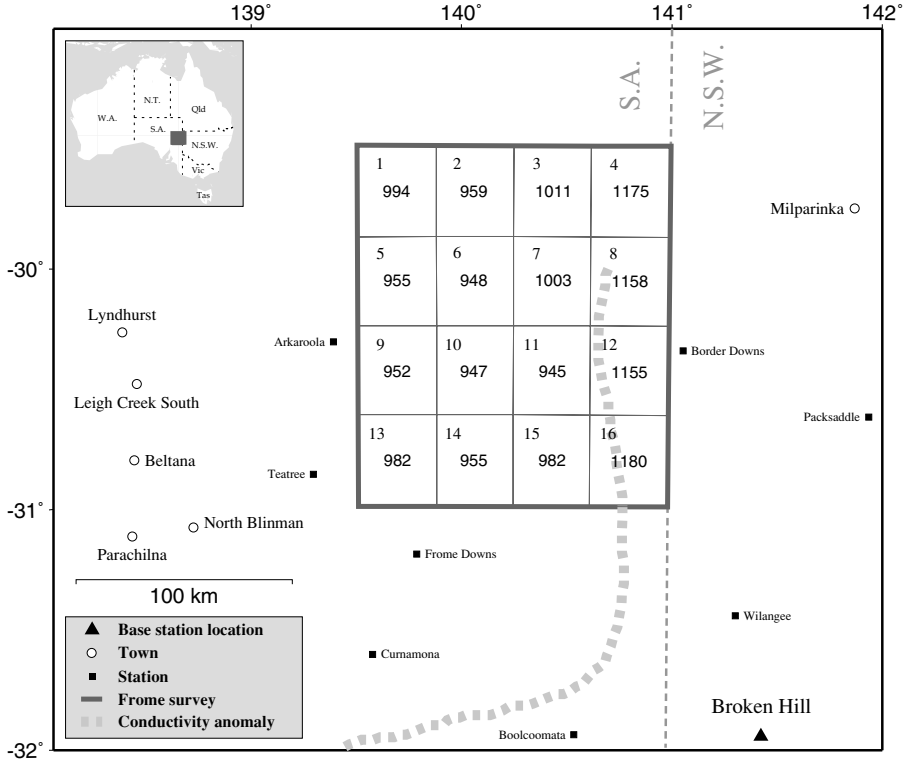

Figure 2. Location of the Frome aeromagnetic survey. The cells used in the present analysis are numbered 1 to 16, and the number of crossover data for each cell is stated (e.g. 994 misfit data for cell No. 1). Broken Hill is the base-station site. The thick dashed line indicates the Flinders electrical conductivity anomaly from magnetometer array studies, after Paul (1994).

components, linked by principles of electromagnetic induction in the Earth, to the total field. For the Frome area, Lilley *et al.* (1999) gave the value of their amphidrome parameter as 4–5, in a range for which value 2 is typical for a highly suppressed area and value 8 is typical for an unsuppressed area.

The Frome area remote from the FCA may thus be expected to experience moderate suppression of magnetic storm activity in measurements of the total magnetic field. Such moderate amphidromic conditions should work in favour of accurate aeromagnetic surveying.

5.1 Base-station data

The base-station magnetometer for the Frome aeromagnetic survey was located at Broken Hill, some 100 km from the survey area. This distance, a result of logistic considerations, is typical in remote parts of Australia. During the Frome survey the base station operated continuously each day that survey operations took place, from before survey flights began after sunrise until the close of operations before sunset. Fig. 3 shows the base-station records for the Frome survey.

5.2 Adjustment of times

The Frome aeromagnetic survey operated in Australian Central Standard Time (CST), which is the local time of South Australia. CST is 9.5 hr ahead of Universal Time. Thus, all basic time data for tie-line crossovers are recorded in CST, as is the base-station time-base. However, the quiet daily magnetic variation, S_q, is commonly modelled as a travelling disturbance, which travels westwards at the rate of the Sun (1° of longitude per 4 min of time). Thus, in an exercise that has as its purpose the determination of S_q as a common signal that occurs at different longitudes at the same local solar times, it is important to adjust all times to a 'local solar time'.

This practice has been followed in the present work, with the 141° meridian of longitude taken as the reference longitude. Thus, a basic t_L value referring to a point **p** that has longitude θ° has been adjusted by subtracting from it an amount $4\,(141-\theta)$ min. Basic t_T values and the base-station times have been similarly adjusted.

The adjustments arising in this way for the Frome survey data are generally a matter of minutes. There is a maximum difference of 8 min in local solar time between the base station at Broken Hill and the western boundary of the survey.

6 EXAMPLES OF RECOVERING THE DIURNAL FUNCTION FOR INDIVIDUAL DAYS

Eventually the space dependence of the misfit data will be examined, by taking the data spatially restricted to cells and unrestricted with regard to time. However, first it is instructive to select, from the whole area, data for individual days. Such data are then unrestricted with regard to space, but restricted with regard to time. A diurnal function is recovered for a specific day, and can be tested by comparison with the variation recorded for that day at the base station.

Subsets of crossover misfits were therefore extracted from the full Frome data set, with each subset containing all the lines and ties flown on some particular day. The crossover points in each subset could be anywhere in the survey area.

The tests were carried out for each of the eight days that ranked highest in the number of misfit data. Of these eight days, the first-ranked held 32 misfit data, and the eighth-ranked held 15 misfit data.

6.1 Individual-day diurnal functions from Fourier series

Fig. 4 presents the diurnal functions thus recovered for the eight days described, using the Fourier series method. The two different times of line measurement and tie measurement at each crossover point are indicated by two black dots on a recovered function. Because two times are associated with each crossover point, the number of dots in each figure is twice the number of crossovers for that day. The full complement of dots is difficult to distinguish in most cases, because many of the times plot close together. The relevant base-station record is shown as a continuous line in each plot.

From the comparison in Fig. 4 of the recovered diurnal functions with the base-station records, it is evident that a segment of the recovered diurnal function that is unconstrained by crossovers may show an excursion that is different from the base-station variation. In Fig. 4, a clear example of this behaviour is shown for day 04/09/95. However, generally the similarities between recovered and base-station variations in Fig. 4 demonstrate the ability of the Fourier method to obtain reasonable diurnal functions from crossover misfits.

The recovered diurnal functions in Fig. 4 represent magnetic field variations obtained for the whole survey area. Minor differences between these and the base-station variations are to be expected if the whole area does not have a uniform electrical conductivity structure. A quantitative comparison of aircraft and base-station variations, intended to exploit such differences, is the subject of Section 7.

6.2 Individual-day diurnal functions from data binning

The same task, of recovering diurnal functions for eight particular days, without applying restrictions of space to the misfit data, has been carried out with the data-binning method. Fig. 5 shows the variations thus recovered, using the same-day crossover data. Bins of width 1 hr have been used. For a diurnal function typically 10 hr in length, bins of this size give 10 unknowns for solution, comparable to the eight unknowns to be determined in the Fourier series method.

Base-station variations are again included for each day, to allow comparison. As can be seen, the data-binning method also produces diurnal functions that are a good match to the base-station daily variations. Comparing Figs 4 and 5 emphasizes the more subdued nature of the data-binning results for these cases. The functions are simply straight lines between successive bins. It would, of course, be possible to use splines, or some similar method, to construct a smooth curve between the successive bin values, but this possibility is not investigated in the present paper.

7 SPATIAL ANALYSIS OF THE DIURNAL FUNCTIONS IN THE FROME AREA

The Frome survey has a uniform crossover pattern and so lends itself to straightforward division into cells of equal size, as shown in Fig. 2. Each cell then contains a similar number of crossovers.

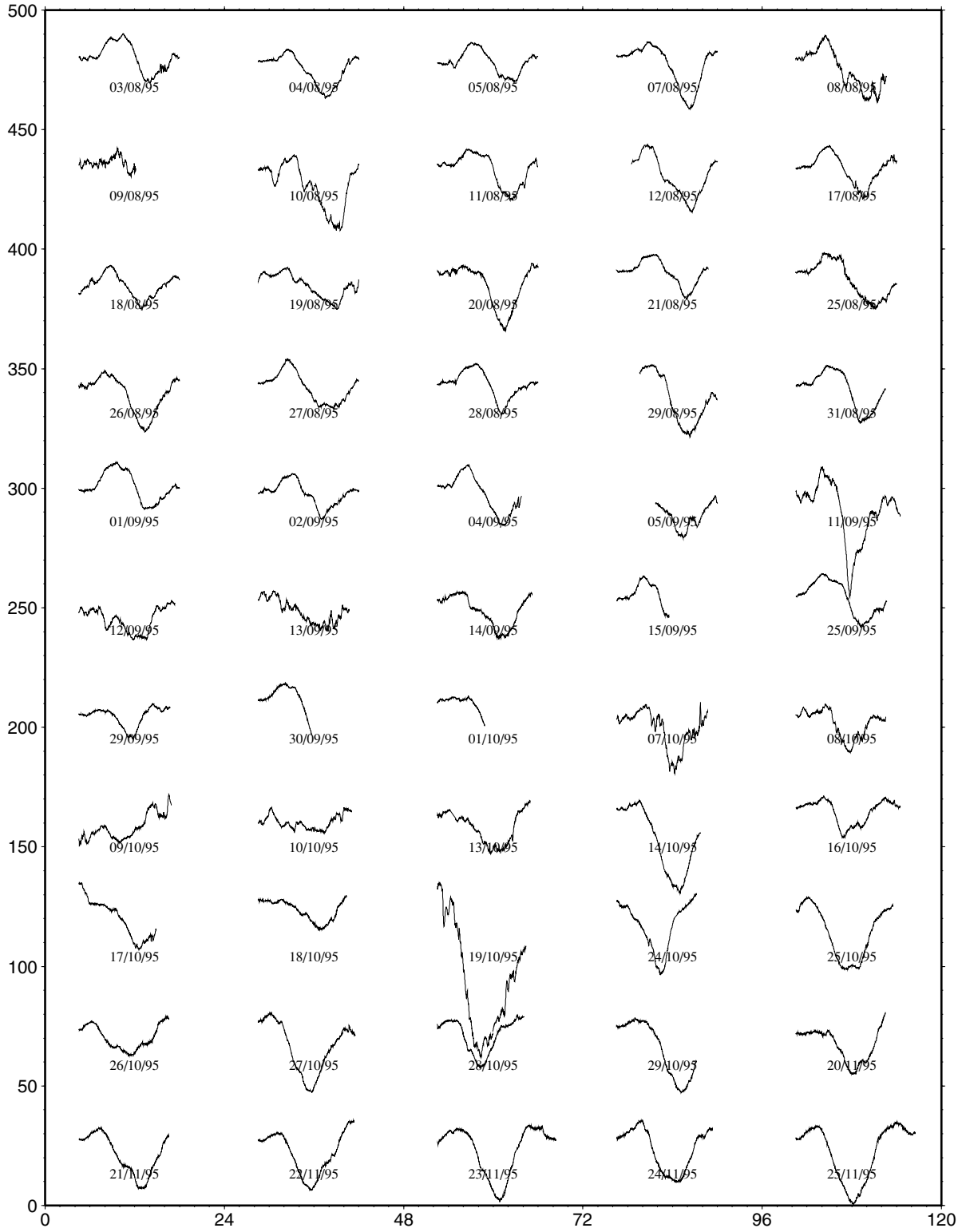

Figure 3. Base-station records for the 55 days during which aeromagnetic measurements were made for the Frome survey. Each day is specified by its date (dd/mm/yy). The horizontal axis is local time (hr), arbitrarily with range 0 to 120 hr. The vertical axis is total field (nT, arbitrarily zero).

The crossover points in each cell are formed from lines and ties flown on various days throughout the survey. Hence, in any cell, the misfit population has contributions from time-variations that occurred on different days. As such, the diurnal functions (both aircraft and base station) derived for each cell will be determined by the daily variations that contributed to the misfits in that cell. The specific influence of a particular daily variation on a recovered diurnal function depends upon the number of misfits formed from data acquired on that day, and on the particular times of those data on that day.

When recovering the aircraft diurnal function for a cell, in addition to the time averaging that occurs due to the variety of

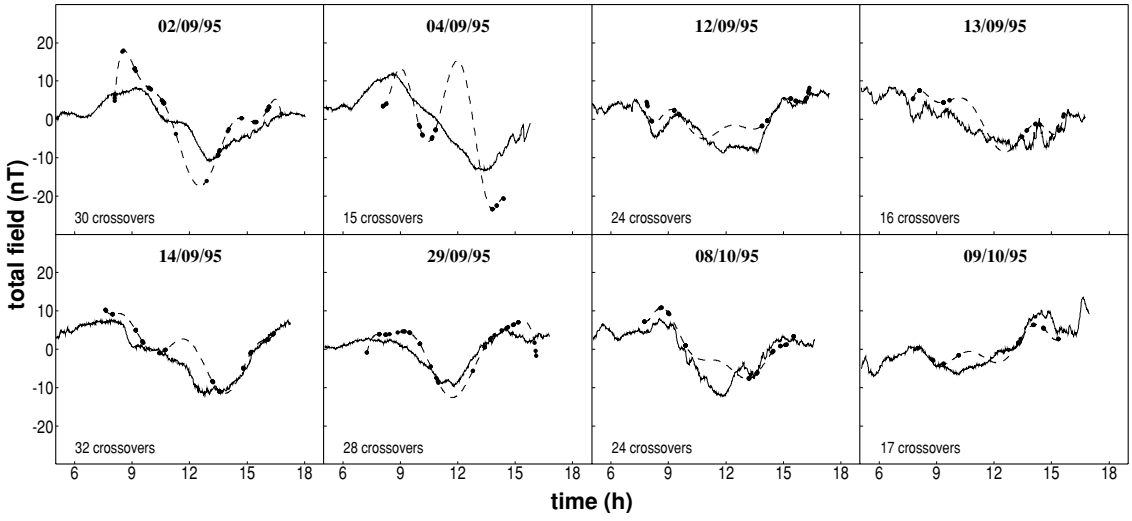

Figure 4. Diurnal functions, for eight particular days, recovered using a Fourier series representation and aeromagnetic crossover misfits from lines and ties all flown on the date (dd/mm/yy) given above each plot. The recovered variation is indicated by a dashed line, and black dots indicate the times at which line and tie measurements were made at crossover points during that day. The full line is the actual base-station record for the day. Time given is local time. All plots in this figure have zero mean value.

days on which the crossovers were flown, there is also a component of space averaging that takes place because the crossover points are distributed over the cell. The base-station diurnal functions, however, are not subject to this space averaging, because the base station is fixed.

Strictly speaking, fewer than 1000 misfits are required for the methods described in Section 3, and possibly smaller cells could be used to give greater spatial resolution. However, in the present exploratory situation a greater number of misfits in each spatial cell is expected to lead to better-determined diurnal functions. The choice of cell size is regarded as sufficient to assess the broad EM response of the area. As a comparison, ground stations on a 40 km by 40 km grid would be quite densely spaced for a reconnaissance magnetometer array study of an area the size of the survey area in Fig. 2.

7.1 Diurnal functions from Fourier series, and residual index values

Fig. 6 shows the aircraft and base-station diurnal functions recovered for each cell of the survey area by the Fourier method. Two main observations may be made about these diurnal functions. First, for any cell, the aircraft and base-station diurnals are very similar. This similarity shows that the time variations within the survey area generally are similar to those at the base station. There are, however, small differences evident between the aircraft and base-station functions for each cell. It is these differences that are analysed for spatial dependence. The second observation from Fig. 6 is that, from cell to cell, the recovered diurnal functions can exhibit substantial differences. Because this cell-to-cell variability is present

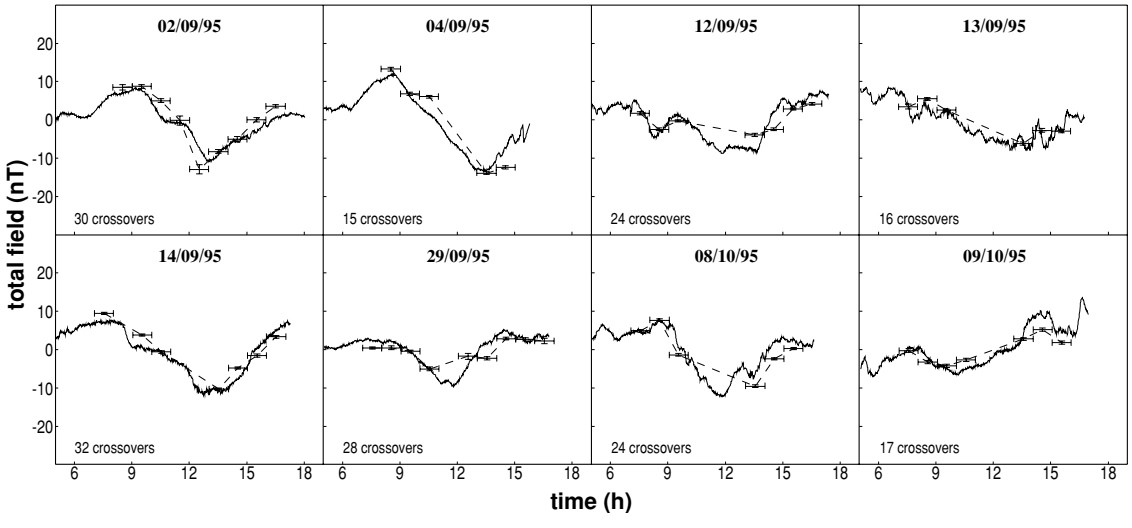

Figure 5. Diurnal functions, for the eight days of Fig. 4, recovered using data binning and aeromagnetic crossover misfits. The misfits are from lines and ties all flown on the particular day. The centres of the recovered bins are joined by straight dashed lines. The horizontal bars indicate bin widths (1 hr). Vertical bars marked at the bin midpoints indicate error bars returned by the SVD method for the bin values. The full line is the base-station record for the day. All plots in this figure have zero mean value.

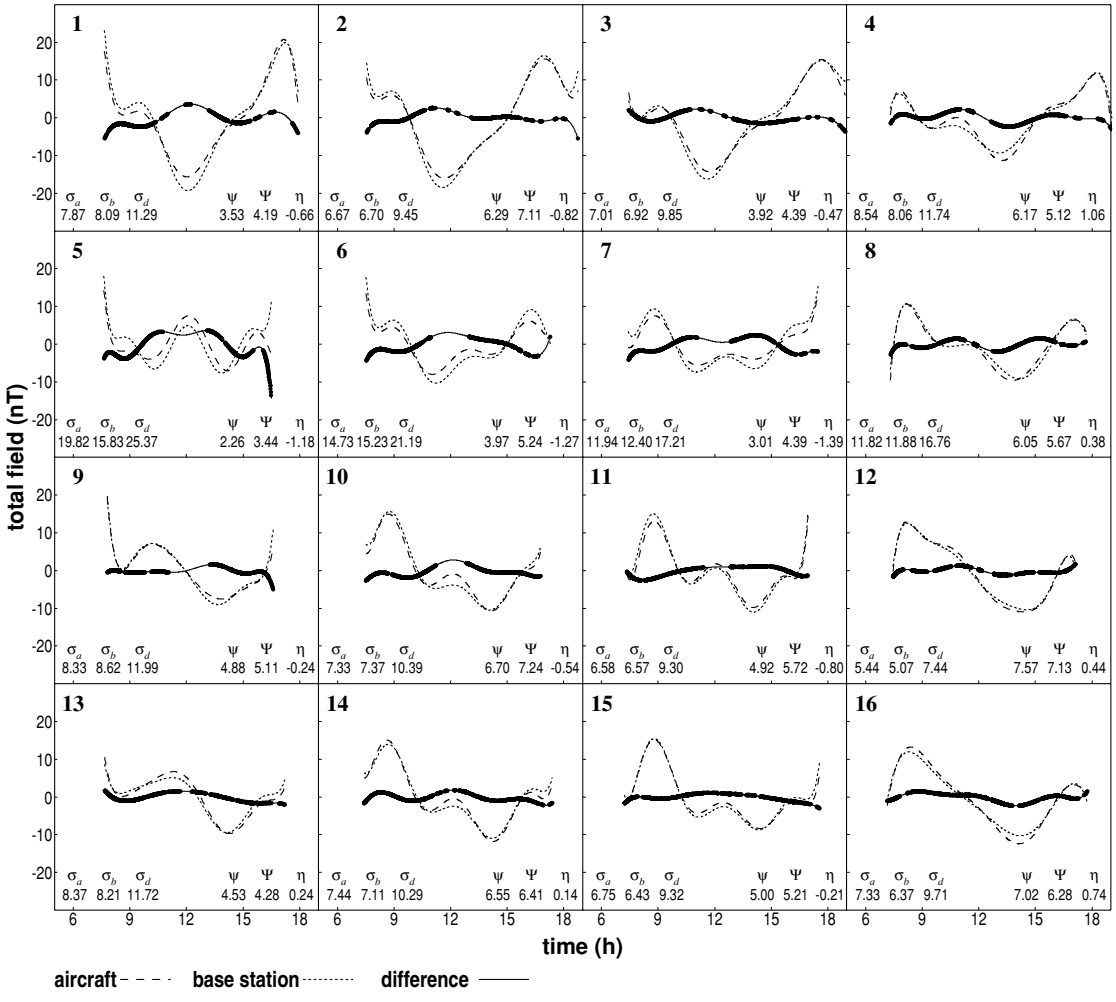

Figure 6. Diurnal functions recovered using the Fourier-series method. The black dots on the residual diurnal function designate the times at which crossover control exists. The number in the top left-hand corner of a panel is the cell number (see Fig. 2). The σ quantities are the error estimates for the aircraft, base-station and difference diurnal functions, as introduced in Section 3.1. The quantities ψ, Ψ and η are explained in the text.

in the diurnal functions recovered for the base station (as well as for the aircraft), it must be due to the different weightings involved in determining the diurnal functions for each cell, rather than being the result of a spatial dependence.

To the bottom right of each plot are the rms measures of the aircraft (ψ) and base-station (Ψ) diurnals, together with the residual index, η. The residual index is computed as set out in Section 4.1. The residual index values are plotted in Section 8 to explore the spatial dependence of the misfit data. Fig. 6 also shows a difference function for each cell, obtained by subtracting the base-station function from the aircraft function point by point.

7.2 Diurnal functions from data binning, and residual index values

The aircraft and base-station diurnal functions recovered using the data-binning method are shown in Fig. 7. Observations made regarding the diurnal similarity within cells, and the differences between cells, in relation to the Fourier-series diurnal functions in Fig. 6 are also pertinent to the data-binning diurnal functions.

The general similarity between the data-binning diurnals and their Fourier-series counterparts is gratifying. There are, however, several instances where 'spikes' are seen in the results from data binning that are not seen in the results from Fourier series; an example is near the middle of the diurnal function for cell 7. This characteristic is thought to result from a bin holding too few misfit data for the reliable determination of its value. In future work, the addition of a criterion regarding the number of data in a bin should prevent such occurrences.

To the bottom right of each plot are the rms measures of the aircraft (ψ) and base-station (Ψ) diurnals, together with the residual index, η. As for those from the Fourier method, the residual index values from data binning are plotted in Section 8 to explore their spatial dependence. Fig. 7 also shows a difference function for each cell, obtained by subtracting the base-station function from the aircraft function point by point.

7.3 Diurnal ratio values

Diurnal ratio values, as introduced in Section 4.2, have been obtained for both the Fourier-series and data-binning diurnal functions. The linear regression method of Press *et al.* (1992, Section 15.3) has been followed.

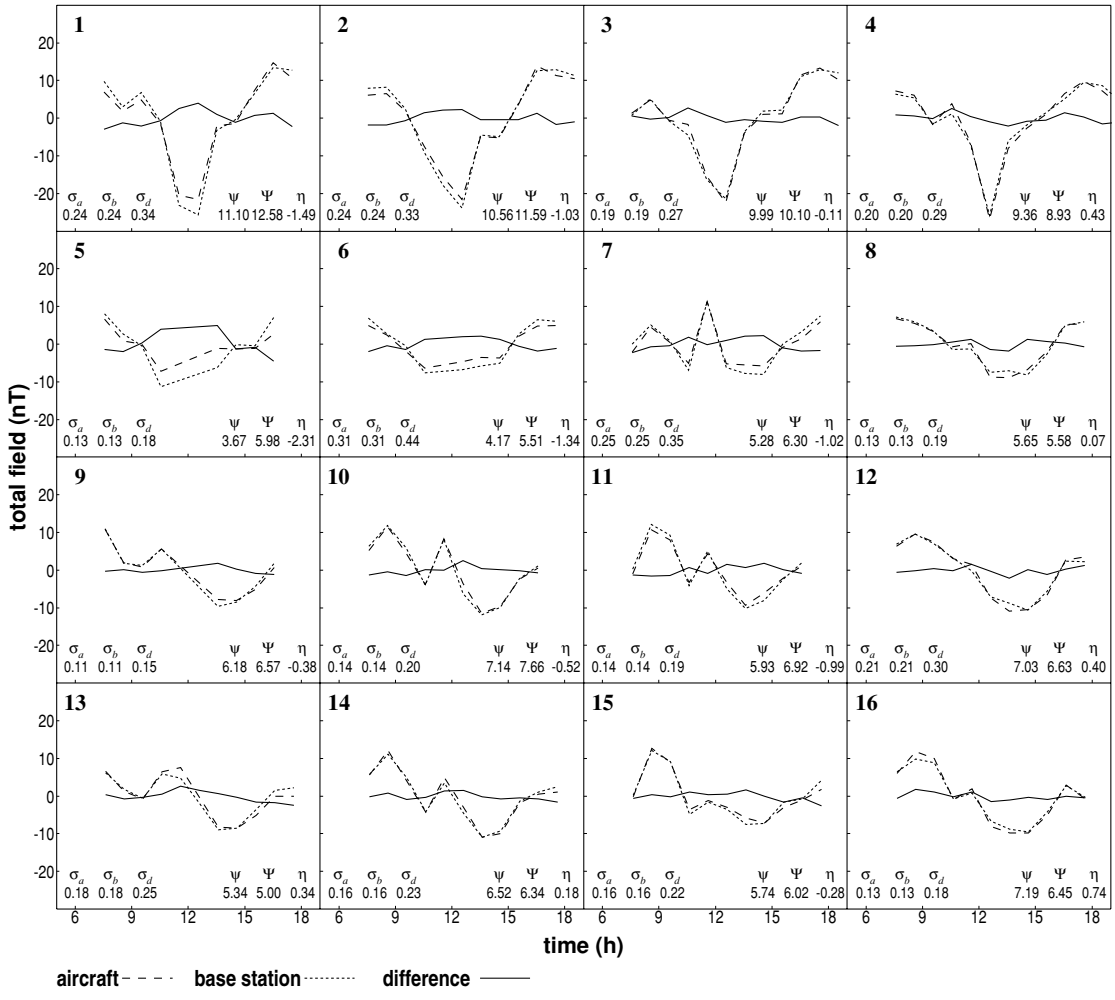

Figure 7. Diurnal functions recovered using the data-binning method. Bin length is 1 hr. Bin values have been plotted at bin midpoints and these midpoints joined by segments of straight lines.

To demonstrate the style of the linear relationships that exist between the diurnal functions, Fig. 8 plots aircraft diurnal function against base-station diurnal function for each cell of the Frome survey, taking the diurnal functions as obtained by data binning. Thus the time-series used for Fig. 8 are those plotted in Fig. 7. Similar plots may be made for the diurnal functions determined by Fourier series.

In Fig. 8, the gradient (denoted by A) of each plot, when multiplied by 100, gives the diurnal ratio for that cell. The correlation coefficient of the two diurnal functions (denoted by C) is a quantitative measure of the linearity of a plot, and in Fig. 8 it can be seen that the values of C obtained are generally close to unity. The spatial variation of the parameter A (as determined by both the Fourier-series and the data-binning methods) is examined below to test the spatial dependence of the misfit data.

8 RESULTS AND DISCUSSION

Fig. 9 summarizes the recovered residual index and diurnal ratio values for each of the two methods, Fourier series and data-binning. The left-hand panels show the actual values of the indices for each cell, and the right-hand panels show those values presented as contour plots. There is excellent agreement between the two residual index patterns. Also, there is excellent agreement between the two diurnal ratio patterns. On the basis of these patterns for the test case of the Frome aeromagnetic survey, both the Fourier and data-binning methods appear to work comparably well.

However, while the formal error estimates for the data-binning results are reasonable, the formal error estimates for the Fourier residual indices are excessive, and the agreement between the patterns in Fig. 9 suggests that the Fourier method errors have been overestimated. Further investigation of them in future studies may clarify this matter. Meanwhile, the data-binning results, and errors, are to be preferred.

The results will be examined for any evidence they may show of electrical conductivity structure, but first it is instructive to consider how various known effects might be predicted to be evident in contour maps such as Fig. 9. On a global scale, the magnetic quiet daily variation, commonly denoted by S_q, has a strong latitudinal dependence. This latitudinal dependence is typically characterized in the three traditional components of magnetic variation, H (magnetic north), D (magnetic east) and Z (vertically down), and it is also present in the total-field

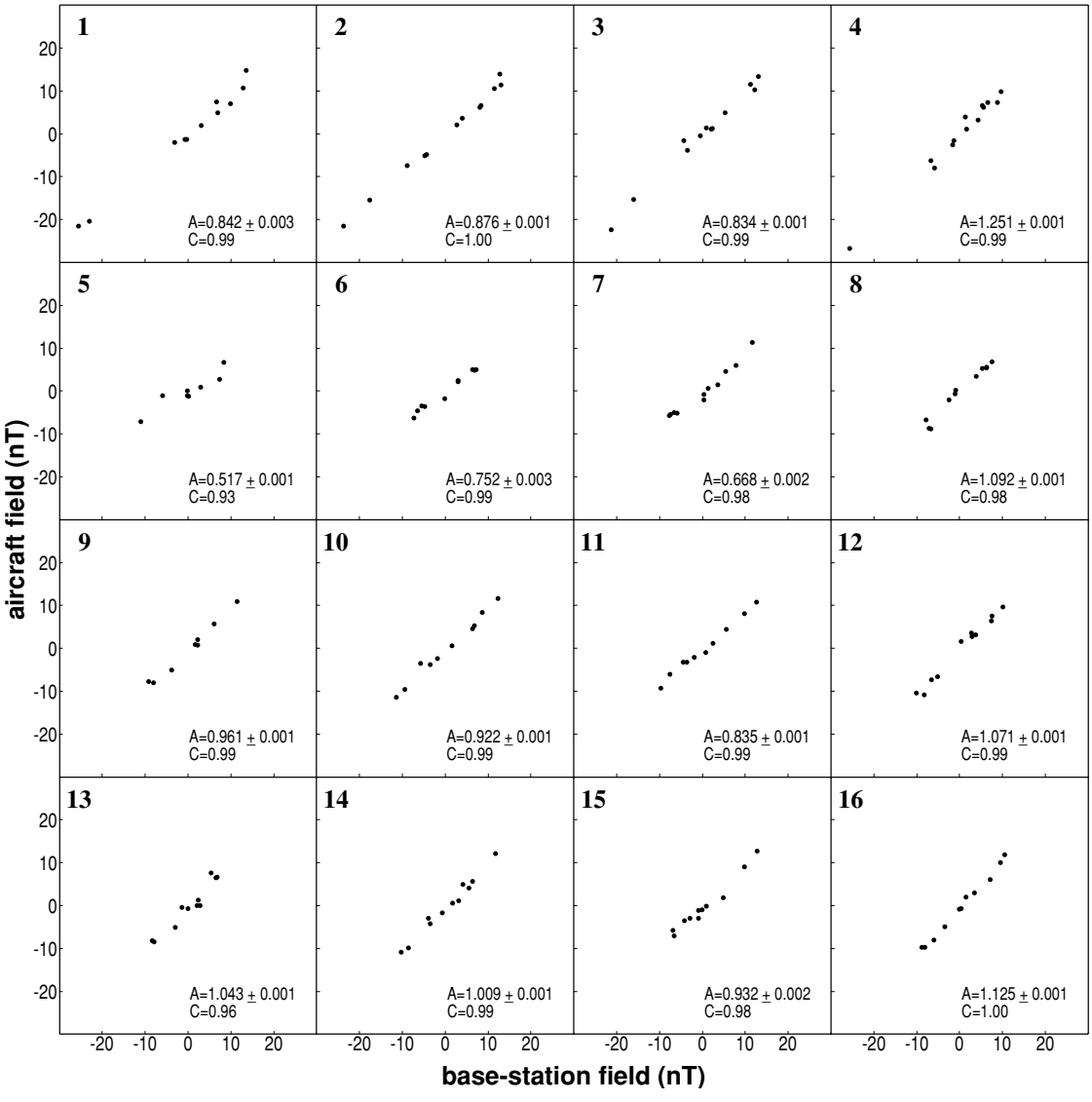

Figure 8. Linear regression analysis of the diurnal functions recovered using the data-binning method. The gradient of the best-fit straight line is denoted by A. The correlation coefficient of the linear regression of the aircraft and base-station diurnal functions is denoted by C.

amplitude, *F*. Hitchman *et al.* (1998a) gave the global latitudinal dependence to be expected for S_q in the total field, and Hitchman *et al.* (1998b) gave its dependence for Australia in particular.

The amplitude of the S_q signal predicted for the Frome area by Hitchman *et al.* (1998b) is shown in Fig. 10. It can be seen that the Frome aeromagnetic survey was carried out over an area where there is a broad maximum in the latitudinal variation of S_q. Over the region under study, therefore, S_q is of effectively uniform amplitude. On the basis of this evidence, source-field effects in Fig. 9 would be expected to be negligible.

The next matter to consider is how local and regional EM induction in the Earth, and especially in heterogeneous electrical conductivity structure, should be evident. Denoting magnetic inclination by I, total-field magnetic variations have a component due to variations in H (as $H \cos I$) and a component due to Z (as $Z \sin I$). They do not, for small variations, have a component directly due to D. However, they may have a component indirectly due to D if D fluctuations induce a Z-component, which then enters F as $Z \sin I$.

The electrical conductivity structure shown in Fig. 2 strikes approximately north. If induced electric current flows along it, then basic considerations predict that such electric current will contribute to anomalous D and Z fluctuations. These in turn will enter the total-fluctuation field as just described. However, it should be remembered that EM induction in electrical conductivity structures is more complicated at the long periods of the magnetic daily variation than at the shorter periods of magnetic substorms in areas of mid-latitude. The reason is that the vertical component of the fluctuation Z, which is approximately nil at shorter periods, will generally be present at long periods, resulting in a complicated interaction of induced Z with normal Z.

Returning now to the plots in Fig. 9, there is a strong enhancement of both the residual index and the diurnal ratio along the eastern edge of the survey area, for both the Fourier and the data-binning results. This feature is thus coincident with the location of the FCA by Paul (1994), as in Fig. 2. To emphasize this point, in Fig. 11 the lower-right panel from Fig. 9 is plotted superimposed upon Fig. 2.

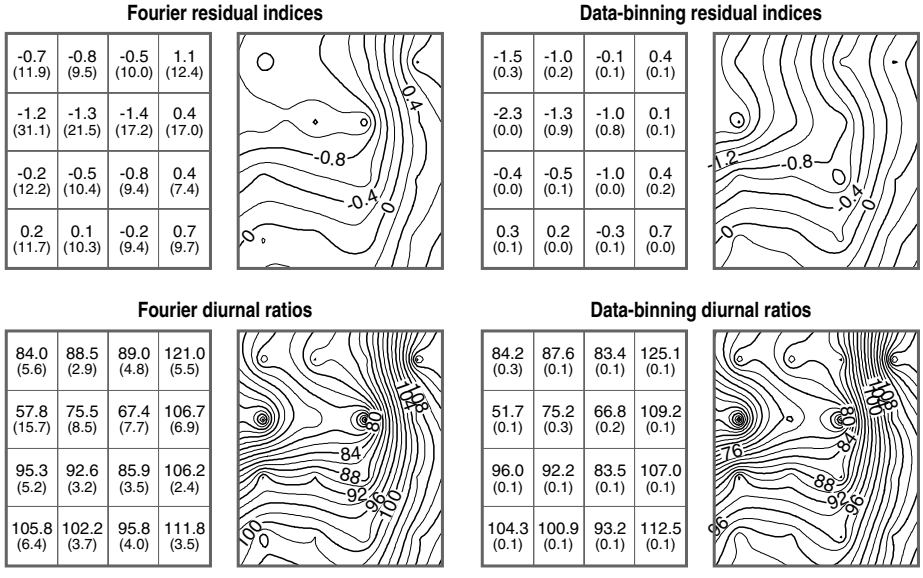

Figure 9. Residual indices and diurnal ratios (as a percentage) recovered for the Frome survey. The values in the left panels are, for each cell, the index value with (in brackets) its estimated standard error. The right panels show the contoured index values.

In Fig. 11 the spatial coincidence of the misfit data pattern with the location of the FCA from ground-station observations is clearly evident. Fig. 11 also shows a region of reduced diurnal ratio in the northwest part of the survey area, and a suggestion of an east–west-trending structure in the southwest. These features are thought to result from complications in the electrical conductivity structure of the area, which were evident in the first analyses of the array data by Gough *et al.* (1972).

9 CONCLUSIONS

The methods developed to test the feasibility of using aeromagnetic misfit data for electromagnetic purposes have produced regional images that are in agreement with known characteristics of the area chosen for study. While as far as possible an objective has been to work in terms of quantitative indices that have been defined, ultimately the present scope of the work is regarded as reconnaissance. Unusual results suggest the presence of electrical conductivity structures, which are then best examined by other detailed follow-up methods (be they ground or airborne).

In principle, such observed data could be modelled, although the frequency response represented is known only in general terms. There may be particular cases, however, where such forward modelling is useful. An example might be to test whether an electrical conductivity structure, suspected to be present on the basis of other data, could indeed be detected by the misfits of an aeromagnetic survey.

The method may thus have wide applications, including over areas of ocean. Aeromagnetic mapping is now frequently carried out over continental shelf areas and other regions with sea-water cover. One of the further case studies described in Hitchman (1999) deals with an aeromagnetic survey from land to continental shelf in eastern Australia, and shows the coast effect to be present in the crossover misfit data.

Aeromagnetic surveys of particular deep-ocean targets also offer distinctive data sets. Thus, for example, it would be interesting to determine whether a modern aeromagnetic survey of the Reykjanes ridge southwest of Iceland, in the style of that described by Heirtzler *et al.* (1966), revealed an electrical conductivity structure associated with the ridge axis.

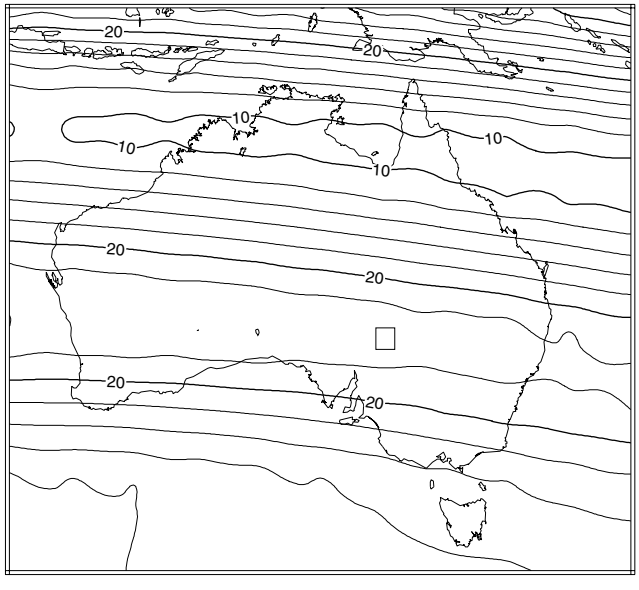

Figure 10. Amplitude of the S_q signal (nT) in the total magnetic field predicted for the Australian region by the model of Hitchman *et al.* (1998a), with the area of the Frome aeromagnetic survey marked by a rectangle.

ACKNOWLEDGMENTS

This paper is based on material in the PhD thesis of APH. The reports of the thesis examiners have contributed significantly to the paper and are much appreciated. We also acknowledge the contributions of two anonymous reviewers of the first version of this manuscript, whose careful comments and recommendations were most beneficial. While the work was in progress we benefited much from discussion on geomagnetic topics with Charles Barton and Wallace H. Campbell.

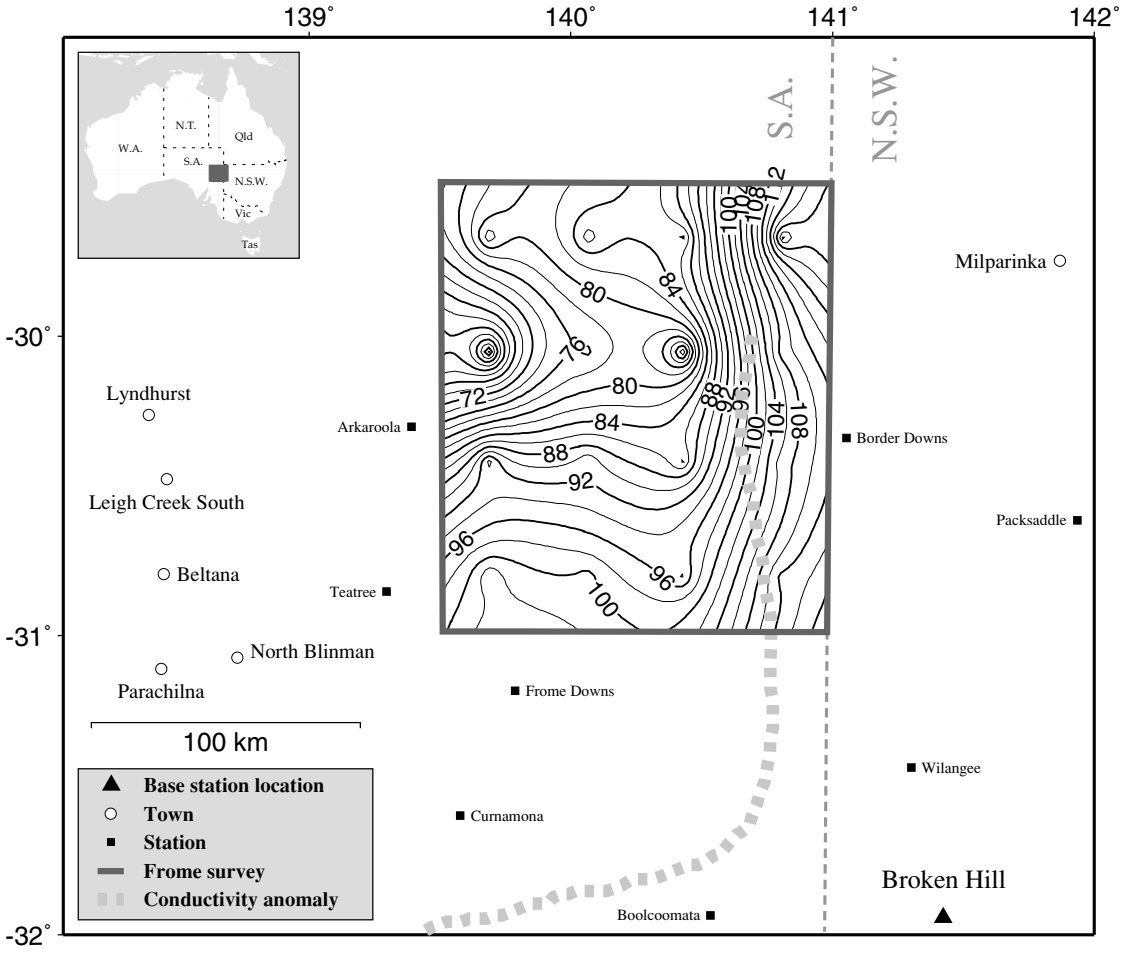

Figure 11. Diurnal ratio results for the Frome area obtained by data binning superimposed upon the location, after Paul (1994), of the Flinders conductivity anomaly.

APH acknowledges the support of an Australian National University Research Scholarship. PRM publishes with the permission of the Chief Executive Officer, AGSO.

REFERENCES

Achache, J., 1977. Les défauts de réduction dans le levé aéromagnétique de la Martinique: existence d'une anomalie de conductivité au sud de l'île, *Ann. Geophys.,* **33,** 217–224.

Campbell, W.H., 1997. *Introduction to Geomagnetic Fields,* Cambridge University Press, Cambridge.

Chamalaun, F.H., 1985. Geomagnetic deep sounding experiment in the central Flinders Ranges of South Australia, *Phys. Earth planet. Inter.,* **37,** 174–182.

Clark, D.A., Schmidt, P.W., Coward, D.A. & Huddleston, M.P., 1998. Remote determination of magnetic properties and improved drill targeting of magnetic anomaly sources by Differential Vector Magnetometry (DVM), *Expl. Geophys.,* **29,** 312–319.

Fanselau, G., 1968. The use of range-differences for the interpretation of conductivity anomalies, *Phys. Earth planet. Inter.,* **1,** 177–180.

Gough, D.I., McElhinny, M.W. & Lilley, F.E.M., 1972. A polarisation-sensitive magnetic variation anomaly in South Australia, *Nat. Phys. Sci.,* **239,** 88–91.

Gough, D.I., McElhinny, M.W. & Lilley, F.E.M., 1974. A magnetometer array study in southern Australia, *Geophys. J. R. astr. Soc.,* **36,** 345–362.

Green, A.A., 1983. A comparison of adjustment procedures for leveling aeromagnetic survey data, *Geophysics,* **48,** 745–753.

Heirtzler, J.R., Lepichon, X. & Baron, J.G., 1966. Magnetic anomalies over the Reykjanes ridge, *Deep Sea Res.,* **13,** 427–443.

Hitchman, A.P., 1999. Interactions between aeromagnetic data and electromagnetic induction in the Earth, *PhD thesis,* The Australian National University, Canberra.

Hitchman, A.P., Lilley, F.E.M. & Campbell, W.H., 1998a. The quiet daily variation in the total magnetic field: global curves, *Geophys. Res. Lett.,* **25,** 2007–2010.

Hitchman, A.P., Lilley, F.E.M., Campbell, W.H., Chamalaun, F.H. & Barton, C.E., 1998b. The magnetic daily variation in Australia: dependence of the total-field signal on latitude, *Expl. Geophys.,* **29,** 428–432.

Horsfall, K.R., 1997. Airborne magnetic and gamma-ray data acquisition, *J. Aust. Geol. Geophys.,* **17,** 23–30.

Langel, R.A. & Whaler, K.A., 1996. Maps of the magnetic anomaly field at Earth's surface from scalar satellite data, *Geophys. Res. Lett.,* **23,** 41–44.

Le Borgne, E. & Le Mouël, J.L., 1975. A conductivity anomaly in the western Mediterranean, *Geophys. J. R. astr. Soc.,* **45,** 939–955.

Lilley, F.E.M., 1975. The analysis of daily variations recorded by magnetometer arrays, *Geophys. J. R. astr. Soc.,* **43,** 1–16.

Lilley, F.E.M., 1982. Geomagnetic field fluctuations over Australia in relation to magnetic surveys, *Bull. Aust. Soc. Expl. Geophys.,* **13,** 68–76.

Lilley, F.E.M., Hitchman, A.P. & Wang, L.J., 1999. Time-varying effects in magnetic mapping: amphidromes, doldrums and induction hazard, *Geophysics,* **64,** 1720–1729.

Luyendyk, A.P.J., 1997. Processing of airborne magnetic data, *J. Aust. Geol. Geophys.,* **17,** 31–38.

Menvielle, M. & Berthelier, A., 1991. The K-derived planetary indices: description and availability, *Rev. Geophys.,* **29,** 415–432.
Milligan, P.R. & Barton, C.E., eds 1997. Transient and induced variations in aeromagnetics, *Aust. Geol. Surv. Org.,* Record 1997/27.
Mitchell, J.N., Milligan, P.R. & Souter, D., 1997. Index of airborne geophysical surveys, 2nd edn, *Aust. Geol. Surv. Org.,* Record 1997/4.
Parkinson, W.D., 1983. *Introduction to Geomagnetism,* Scottish Academic Press, Edinburgh.
Paul, S.K., 1994. Geomagnetic induction study of the Adelaide Geosyncline, *PhD thesis,* The Flinders University of South Australia, Adelaide.
Press, W.H., Teukolsky, S.A., Vetterling, W.T. & Flannery, B.P., 1992. *Numerical Recipes in C, The Art of Scientific Computing,* 2nd edn, Cambridge University Press, Cambridge.
Ravat, D., Langel, R.A., Purucker, M., Arkani-Hamed, J. & Alsdorf, D.E., 1995. Global vector and scalar Magsat magnetic anomaly maps, *J. geophys. Res.,* **100,** 20 111–20 136.
Reeves, C.V., 1993. Limitations imposed by geomagnetic variations on high quality aeromagnetic surveys, *Expl. Geophys.,* **24,** 115–116.
Richardson, L.M., 1996. Frome (Frome and southern Callabonna 1:250000 sheet areas), airborne geophysical survey, 1995—operations report, *Aust. Geol. Surv. Org.,* Record 1996/20.
Riddihough, R.P., 1971. Diurnal corrections to magnetic surveys—an assessment of errors, *Geophys. Prospect.,* **19,** 551–567.
Sander, E.L. & Mrazek, C.P., 1982. Regression technique to remove temporal variation from geomagnetic survey data, *Geophysics,* **47,** 1437–1443.
Schmidt, P.W., Clark, D.A., Coward, D.A. & Huddleston, M.P., 1993. Development and application of Differential Vector Magnetometers, *Expl. Geophys.,* **24,** 123–126.
Whellams, J.M., 1996. Spatial inhomogeneity of geomagnetic fluctuation fields and their influence on high resolution aeromagnetic surveys, *PhD thesis,* The Flinders University of South Australia, Adelaide.
White, A. & Polatayko, O.W., 1985. Electrical conductivity anomalies and their relationship with the tectonics of South Australia, *Geophys. J. R. astr. Soc.,* **80,** 757–771.
Yarger, H.L., Robertson, R.R. & Wentland, R.L., 1978. Diurnal drift removal from aeromagnetic data using least squares, *Geophysics,* **43,** 1148–1156.

APPENDIX A: CROSSOVER MISFITS

Fig. A1 shows the magnitude distribution of the crossover misfits (some 16 301 in total) for the Frome survey. The distribution is a slightly peaked Gaussian distribution with a positive kurtosis that is, however, small (Press *et al.* 1992, Section 14.1). The symmetry of a distribution about its mean is measured by the skew, and the small positive value of skew for the Frome data represents a slightly longer tail of positive misfits. These kurtosis and skew characteristics of the misfit data may result from some particular strategy followed in obtaining the tie data. For example, sometimes ties are flown systematically early in the morning, or as far as possible on the same day, etc.

The essentially Gaussian nature of the misfit population, notwithstanding the variety of effects that can contribute to misfits, is pleasing to note. Subsequent analysis can be made with confidence in the integrity of the data.

Fig. A2 shows the relationship between misfit and magnetic activity level. Every misfit was assigned a *Kp* index, defined as the greater of the two *Kp* indices measured at the time of the line and tie (for a description of *Kp* indices, see Menvielle & Berthelier 1991). The misfit population was then subdivided

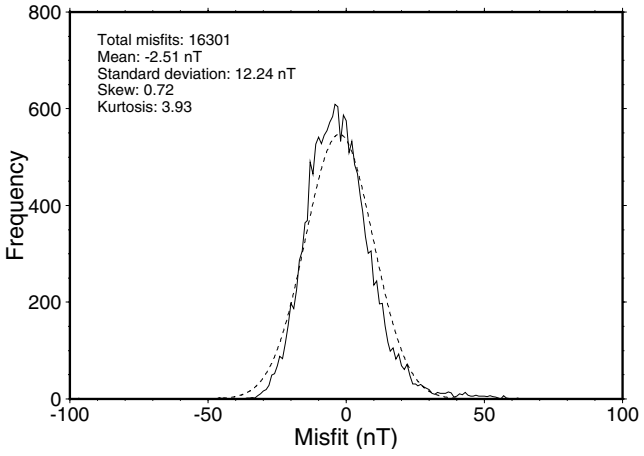

Figure A1. Magnitude distribution of the Frome crossover misfits. The dashed line represents a Gaussian distribution.

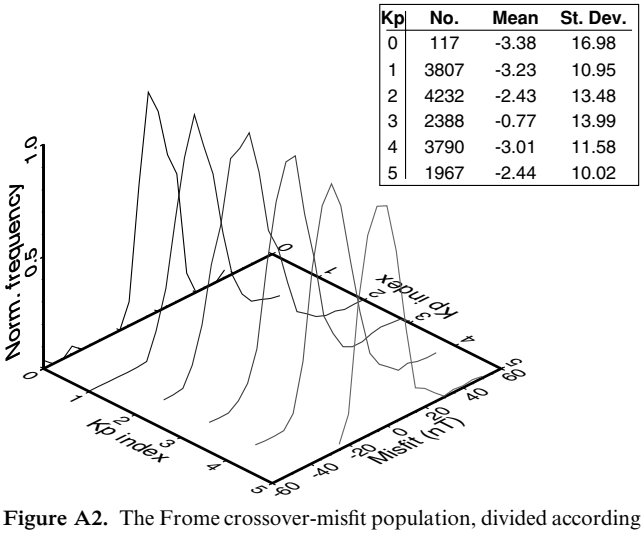

Kp	No.	Mean	St. Dev.
0	117	-3.38	16.98
1	3807	-3.23	10.95
2	4232	-2.43	13.48
3	2388	-0.77	13.99
4	3790	-3.01	11.58
5	1967	-2.44	10.02

Figure A2. The Frome crossover-misfit population, divided according to the greater *Kp* index at the times of the line and tie measurements. Histograms are obtained using 5 nT misfit bins. The inset table shows the number of misfits and their mean and standard deviation in each sub-population.

according to this *Kp* index, and histograms computed and normalized for each subpopulation. Of particular interest was whether the statistical nature of subpopulations is influenced by the *Kp* index, in particular whether increased magnetic activity resulted in larger crossover misfits. Such an occurrence would be expected to be represented by higher standard deviations for the subpopulations with higher *Kp* indices.

While the present paper is concerned with obtaining a long-period estimate, an important conclusion from Fig. A2 is that increasing magnetic activity appears to have little observable effect on the misfit. Possibly this result is a consequence of the moderate amphidromic circumstances of the Frome area, referred to in Section 5. These circumstances cause a suppression, in the Frome and Broken Hill areas, of the increased magnetic activity, which would otherwise generally accompany higher *Kp* indices.